Modelling the photooxidation of ULP, E5 and E10 in the CSIRO smog chamber

Stephen J. White[a,b], Merched Azzi[a,*], Dennys E. Angove[a] and Ian M. Jamie[b]

[a] CSIRO Energy Technology, Private Mail Box 7, Bangor, NSW 2234, Australia.

[b] Department of Chemistry and Biomolecular Sciences, Macquarie University, NSW 2109, Australia.

[*] Corresponding author. Address: Private Mail Box 7, Bangor NSW, 2234.

Tel: +61 2 9710 6870; Fax: +61 2 9710 6800. Email: Merched.Azzi@csiro.au

Abstract

The photooxidation of fuel vapour was investigated in a smog chamber and simulated using three chemical mechanisms, the Master Chemical Mechanism (MCMv3.1), SAPRC-99 and the Carbon Bond chemical mechanism (CB05). Three varieties of fuel were used, unleaded petrol (ULP) and two ULP-ethanol blends which contained 5% and 10% ethanol (E5, E10). The fuel vapours were introduced into the chamber using two methods, by injecting the vapours from wholly evaporated fuel directly, and by injecting the headspace vapour from fuel equilibrated at 38 °C. The chamber experiments were simulated using the selected mechanisms and comparisons made with collected experimental data.

The SAPRC-99 mechanism reproduced $\Delta(O_3\text{-NO})$ more accurately for almost all fuel types and injection modes, with negligible model error for both injection modes. The average model error for MCM simulations was -16% and for CB05 the average model error was -34%. The predictions for the CB05 mechanism varied depending on injection mode, the $\Delta(O_3\text{-NO})$ model error for wholly evaporated experiments was -44%, compared to -24% for headspace vapour experiments. The difference in aromatic content between experiments of different injection modes was likely to be the cause of the difference in model error for CB05. The model error for all headspace experiments was dependent upon the initial carbon monoxide concentrations.

The results for $\Delta(O_3\text{-NO})$ were matched by the prediction of other key products, with formaldehyde predicted to within 20% by both SAPRC and the MCM. The addition of ethanol to the base SAPRC mechanism altered the predictions of $\Delta(O_3\text{-NO})$ by less than 2%. Changes observed in the concentrations of formaldehyde and acetaldehyde were consistent with the expected yields from ethanol oxidation.

Keywords: Chemical mechanisms, ethanol, SAPRC, MCM, CB05

Introduction

The emission into the troposphere of volatile organic compounds (VOCs) can contribute to the air pollution load in the lower atmosphere (Beer, 2001). Some compounds such as benzene and 1,3-butadiene are directly emitted whereas other compounds such as ozone, formaldehyde and acetaldehyde can be formed by secondary processes (Atkinson, 2000; Finlayson-Pitts and Pitts, 1997). Within urban environments, the major source of VOC emissions is fuel evaporation and combustion (Watson et al., 2001).

Alternative fuel sources such as ethanol are being increasingly used in blends with fossil fuels due to the negative impact of fossil fuel-based emissions on radiative forcing. As fuel evaporation and combustion is an important component of VOC emissions in urban areas, there is a need to determine the effect that ethanol usage in fuel will have on both primary and secondary air pollutants.

The inclusion of ethanol into fuel in low concentration blends (E10, E15, E22) has been shown to lower the direct exhaust emission of ozone-forming VOCs and carbon monoxide from combustion engines, while increasing the atmospheric concentrations of acetaldehyde (Schifter et al., 2001). In Brazil, where the use of ethanol in fuel has been long established, the ambient concentrations of ethanol and acetaldehyde have increased, while fuel-based VOC concentrations have decreased (Nguyen et al., 2001).

Environmental chambers provide controlled conditions under which the photooxidation of VOCs can be studied. The ability of chemical mechanisms to reproduce ozone and other smog formation products in these experiments can be evaluated. A number of chamber studies have been performed relating to fuel and ethanol usage: using diesel exhaust (Geiger et al., 2002), ethanol containing fuels (Carter et al., 1999; Pereira et al., 2004) and captive air experiments from areas where oxygenated fuels are used (Grosjean and Grosjean, 1998; Gasca et al., 2004).

A study carried out on the health impacts of ethanol blend petrol (CSIRO and Orbital Engine Corporation Australia, 2008) showed that based on smog chamber experiments for wholly evaporated fuel, the ozone produced by ULP was higher than that produced by E5 and E10. For headspace vapour, the amount of ozone formed from ULP was no different to that formed during E5 and E10 experiments. In addition, the concentration of ozone formed by the wholly evaporated fuel vapour was significantly higher than that formed from the headspace vapour.

In this work, chemical mechanism modelling of evaporated fuel vapour chamber experiments performed in the health impacts of ethanol blend petrol study (CSIRO and Orbital Engine Corporation Australia, 2008) are presented. These experiments were simulated by three chemical mechanisms to evaluate their performance in predicting ozone and other major smog formation compounds, and to assess the impact of ethanol on mechanism predictions.

Experimental

Smog chamber description and instrumentation

Experiments were carried out in the CSIRO indoor environmental chamber which has been described previously (Hynes et al., 2005; Angove et al., 2006). The chamber has a volume of 18 m^3 and is lined with FEP Teflon film. It is fitted with two UV-A lighting modules, each containing 40 black-light tubes (36W Sylvania Blacklight Blue 350). These lamps emit radiation over the range 350-390 nm, with peak intensity at 366nm.

The concentrations of NO, NO_y and O_3 were determined in-*situ* as previously described (Hynes et al. 2005). The concentrations of O_3, CO, formaldehyde, PAN, ethanol and formic acid were determined using FTIR (Nicolet Magna 550). FTIR spectra were obtained at a resolution of 1 cm^{-1} and were the coaddition of 512 scans obtained over 9 minutes. Fitting of these spectra to species of interest was performed using MALT (Griffith 1996) with the use of the HITRAN database for most species (Rothman et al. 2005), and absorption spectra for ethanol (Chu et al. 1999). Further information is available in Table A1 in supplementary data.

The concentration of VOCs was determined by canister grab samples which were analysed using GC-FID and a certified 100 ppbv USEPA TO-15/PAMS hydrocarbon mixture (CSIRO and Orbital Engine Corporation Australia, 2008). Those species present in the vapour but not in the certified mixture were identified by retention time comparisons

with fuel speciation analyses performed independently by Intertek Testing Services according to ASTM D6730-01. Air was sampled into 4 L canisters for approximately 40 seconds, with one sample being taken at the beginning of each experiment to determine initial VOC concentrations. A list of the VOC species identified is shown in Table A2 in supplementary data. The method detection limit for VOCs was in the range of 0.1-1.4 ppbv. Formaldehyde, acetaldehyde and acetone were measured using DNPH cartridges (Waters Corporation), preceded by an ozone scrubber cartridge (Waters Corporation), and were analysed using HPLC according to California Air Resources Board method MLD 104 (CSIRO and Orbital Engine Corporation Australia, 2008). For each experiment, either two or four cartridge samples were collected over a period of 20-30 minutes each at a flow rate of 1.2 L min^{-1}, and analysed within a week of collection. The detection limit was 1 ppbv with a maximum standard deviation of 10%.

Chamber Experiments

Experiments were performed using evaporated fuel mixtures injected in two different modes. The first injection mode used wholly evaporated fuel, where 19.0 ± 0.5 μL of chilled fuel was injected in a glass bulb through which nitrogen was gently streamed into the chamber. The bulb was gently heated during the 10 minute injection. The second injection mode was performed using headspace equilibrated fuel. The headspace samples were prepared by placing 20 mL of fuel in a 200 mL reinforced bottle inserted into a purpose-designed aluminium jacket and equilibrated for 2 hours at 38 °C. Sample volumes of 8 mL of the headspace vapour were then injected directly into the chamber using a gas-tight syringe. The injection volumes used ensured similar initial VOC concentrations of 1.2 ± 0.2 ppmvC for both injection modes.

A total of 12 smog chamber experiments were carried out using three different fuels, unleaded petrol (ULP) and two ethanol blends (E5 and E10), allowing a replicate of each experiment to be performed. In between experiments the fuel was stored at -20°C. The same batch of petrol was used to make up the ULP and ethanol blends (CSIRO and Orbital Engine Corporation Australia, 2008). Analysis of the sulphur content of the fuels used in these experiments showed that the maximum sulphur concentration in the gas phase for wholly evaporated experiments was less than 0.1 ppbv. As sulphur concentrations were also expected to be lower than 0.5 ppbv in headspace experiments, the sulphur concentration was considered comparatively low enough to exclude for modelling purposes.

Comparison of fuel composition for two headspace and two wholly evaporated experiments is shown in Fig. 1. The wholly evaporated experiments are characterised by higher concentrations of aromatic hydrocarbons and large alkanes, while the headspace experiments contain higher concentrations of products with higher vapour pressures such as short-chained alkanes and alkenes. The lower concentration of VOCs in the ethanol blends reflects the lower concentration of ULP due to ethanol content.

In each experiment, nitric oxide (1.09 ± 0.05% in N_2) was injected to an initial NO_x concentration of 133 ± 3 ppbv, giving an initial VOC/NO_x of 8.4 ± 0.7 (ppmC / ppmN). Water (Milli-Q purified) was injected such that the initial relative humidity was approximately 50% at 296 °K (Center 313 Humidity/Temperature Meter). All experiments were performed for a period of 6 hours irradiation. The light intensity used for these experiments was equal to a J_{NO2} of 0.45 ± 0.03 min^{-1}.

For all experiments a flux of nitrous acid (HONO) was provided constantly into the chamber at 1.5 ± 0.5 ppbv $hour^{-1}$ by a HONO generator (Carter and Malkina, 2002). The generator was activated 10 minutes before the start of each experiment. The HONO flux rate was measured in two separate experiments by injecting HONO constantly into a dark chamber for five hours. The chamber contents were regularly mixed and the concentration steadily increased and was measured by a NO_y chemiluminescent analyser operated at the other end of the chamber. The concentration was also determined by FTIR measurements, using a reference spectrum (Hanst and Hanst 1993) and the peak at 852 cm^{-1}. The reference spectrum was quantified by using absorption data for the peak at 1263 cm^{-1} (Syomin and Finlayson-Pitts 2003).

Modelling

Mechanism descriptions

Three chemical mechanisms were used to model the chamber experiments: the Master Chemical Mechanism (MCMv3.1), the SAPRC mechanism (SAPRC-99) and the Carbon Bond chemical mechanism (CB05).

The MCM represents the most explicit chemical mechanism for tropospheric VOC oxidation available (Jenkin et al., 1997). The most recent update to the MCM incorporated significant updates to the aromatic hydrocarbon mechanism (Bloss et al., 2005). SAPRC-99 is a detailed tropospheric mechanism which has been evaluated against over 1700 experiments performed at several different smog chambers (Carter, 2000). SAPRC does

not model the oxidation of every VOC explicitly such as the MCM, but uses a lumped approach to assign VOCs to a smaller number of reactive species. The Carbon Bond mechanism is a lumped molecule mechanism that has been used in ambient modelling studies (Luecken et al., 2008). The most recent version, CB05, has been evaluated against chamber studies using sunlight and blacklights as irradiation sources (Yarwood et al., 2005).

Treatment of ethanol oxidation in the mechanisms

The treatment of ethanol by the mechanisms was important given that ethanol constitutes a significant proportion of the initial VOC mixture in experiments using ethanol blended fuels. In the MCM and CB05, ethanol was represented as an explicit species. Using SAPRC ethanol could be explicitly represented for single hydrocarbon experiments (Carter, 2000). However for implementation in chamber experiments using hydrocarbon mixtures, the lumping protocol used by the SAPRC software was used to lump ethanol as well as all other hydrocarbons to a smaller number of reactive species. In each mechanism ethanol or its equivalent lumped analogue was removed only through reaction with the OH radical.

A comparison of the ethanol reactivity with OH and the product yield is shown in Table 1. For SAPRC ethanol as it is treated by the adjusted product mechanism is shown, but this is not reflective of how ethanol is treated in the lumped simulations. The reaction rates are equivalent between the mechanisms, although the temperature dependence of the rate in the SAPRC mechanism is incorrect (Atkinson et al., 2006).

VOC Speciation

The initial concentration of up to 230 hydrocarbons was determined using GC-FID. Carbonyl concentrations were measured for a select number of experiments, but the initial concentrations were always below the detection limit. The initial concentration of ethanol was determined for those experiments using ethanol blends, and was between 30 and 60 ppbv. The concentration of other oxygenated VOCs was not determined, but was assumed to be low enough to not affect reactivity significantly. Initial concentrations of methane (1-3 ppmv) and CO (0.1-0.8 ppmv) were also measured for each experiment.

To conform to the structure of each particular mechanism, the method of initial VOC speciation varied. For the MCM many of the hydrocarbons were explicitly represented in the mechanism. For species that were not present in the MCM an equivalent

surrogate species was determined, consistent with regional-scale modelling of ambient scenarios using the MCM (Utembe et al., 2005). In the SAPRC mechanism, each VOC was assigned a detailed model species name (DMS) (Carter 2000), with some species sharing the same DMS. These DMS names were used as VOC input for the mechanism simulations. A full list of speciation for both mechanisms is provided in supplementary data. For CB05, initial concentrations were determined by using the lumped structure approach (Yarwood et al. 2005).

Auxiliary mechanism

The wall mechanism for the CSIRO chamber has been determined previously (Hynes et al., 2005). Changes can occur to chambers over time which can affect the auxiliary mechanism (Carter et al., 2005) and therefore some of the key reaction rates were re-evaluated (Table 2). Consistent with recent work showing HONO formation from the chamber walls (Rohrer et al., 2005), the main light-induced radical formation was changed from OH and NO_2 to HONO, and the rate determined using clean air and CO irradiation experiments.

A reaction rate of OH to HO_2 was included to match radical formation in clean air runs, assumed to be from the reaction of background hydrocarbons (Carter and Lurmann, 1991). Although the hydrocarbon concentration was measured explicitly both in the previous wall characterisation and these experiments, this rate was included but was found to have only a small effect on ozone predictions for these experiments.

All experiments were performed with a constant HONO flux of 1.5 ppbv $hour^{-1}$. For all experiments the initial HONO concentration was set at 0.7 ppbv, consistent with 10 minutes of HONO injection before experiment initiation and background concentrations present as a result of NO_x injection.

Chamber simulations

Each mechanism was run as a self-contained box model, with initial concentrations specified for each experiment. The wall mechanism, light emission profile and HONO injection rates were consistent for all mechanisms and experiments, with temperature updated every 5 minutes. The MCM was run utilising the FACSIMILE software package, SAPRC was run using the SAPRC software (Carter 2000) and the CB05 mechanism was run as a self contained box model, adapted from the Chemical Transport Modelling (CTM) program (Cope et al. 2004).

Method of comparison

The primary method of assessing the oxidative capacity of a smog chamber experiment is to use $\Delta(O_3\text{-NO})$ (Johnson 1983; Carter and Atkinson, 1987), where $\Delta(O_3\text{-NO}) = ([O_3]_t - [O_3]_0) - ([NO]_t - [NO]_0)$. This term represents the ability of the system to form ozone in the presence of NO, by including the conversion of NO to NO_2. The model error for the simulations was calculated as $(\Delta(O_3\text{-NO})_{mod} - \Delta(O_3\text{-NO})_{exp}) / \Delta(O_3\text{-NO})_{exp} \times 100\%$. The model error was calculated in this work after six hours, or the end of experiment.

Results

Experimental ozone formation

The experimental results for these experiments have been presented elsewhere (CSIRO and Orbital Engine Corporation Australia, 2008). In summary, the wholly evaporated fuel vapours produced more ozone than headspace vapours (Fig. 2). This increase was consistent with the higher concentration of aromatic hydrocarbons in the wholly evaporated fuel. The was negligible difference in $\Delta(O_3\text{-NO})$ between headspace fuel varieties due to similar non-ethanol VOC concentrations (Fig. 1). However for wholly evaporated fuel the final $\Delta(O_3\text{-NO})$ concentration was negatively correlated to the ethanol concentration in the fuel, which is consistent with the 5 and 10% drop in total non-ethanol VOC concentration for E5 and E10 fuel respectively. These results are consistent with ethanol having only a minor impact on ozone formation over six hours irradiation.

HONO generation rate

The injection of HONO was a large source of OH radicals during the experiment, and therefore the rate of flux was vital in determining the radical balance and reactivity of the system. The impact of the experimental uncertainty in the HONO generation rate on $\Delta(O_3\text{-NO})$ predictions was tested for a headspace evaporated experiment (Fig. 3) and wholly evaporated experiment (Fig. 4). The shaded regions represent the predictions between the upper bound of HONO flux at 2.0 ppbv $hour^{-1}$ and the lower bound at 1.0 ppbv $hour^{-1}$. The effect was not consistent across the chemical mechanisms, with the MCM less sensitive to changes in the HONO flux rate than the other two mechanisms. The lower sensitivity of the MCM to HONO injection rate changes was related to the reaction rates of HONO in each mechanism. The rate of formation of HONO from OH and NO was quicker in the MCM, while the photolysis rate was slower than the other mechanisms. Both of

these favoured higher concentrations of HONO relative to NO and OH in the MCM compared to SAPRC or CB05 (supplementary data). As such, changes to the HONO flux rate will have a larger effect on SAPRC or CB05 than on the MCM. The maximum variability in $\Delta(O_3\text{-NO})$ at the end of the experiments is no more than ± 6 % for the upper and lower bounds of the HONO flux rate, independent of the injection mode. The HONO generation rate was therefore set as 1.5 ppbv $hour^{-1}$ for all experiments.

Experimental $\Delta(O_3\text{-NO})$ error

The final $\Delta(O_3\text{-NO})$ model error for headspace and wholly evaporated experiments is summarised in Table 3. For ULP and E10 fuel experiments using headspace vapours, SAPRC reproduces $\Delta(O_3\text{-NO})$ more accurately than the MCM, with the MCM simulations slightly more accurate than CB05 simulations. The exception is the average model error for E5 fuel using headspace injection, which was more accurately predicted by the MCM. The E5 headspace experiments had increased positive bias relative to results from E10 and ULP headspace experiments for all mechanisms.

The final model errors for the headspace vapour experiments varied due to the initial concentration of carbon monoxide (Fig. 5). As both E5 experiments had higher initial carbon monoxide, this was reflected in the average model error for E5. Under high-NO_x and high-OH radical conditions, similar to those present in these chamber experiments, the reactions of CO with OH will readily form HO_2 which reacts with NO to regenerate OH. The model error dependence on CO was reflected in the predictions of maximum HO_2 by SAPRC, which was correlated to the initial CO concentration (Fig. 5). This demonstrates the importance of the reaction of the hydroxyl radical and carbon monoxide on radical formation in these experiments.

The final $\Delta(O_3\text{-NO})$ model error for wholly evaporated experiments is shown in Table 3. The SAPRC mechanism reproduces $\Delta(O_3\text{-NO})$ more accurately than the other two mechanisms, with the MCM more accurate than CB05. Unlike headspace experiments the initial carbon monoxide concentration, which varied between 0.1 and 0.35 ppmv, made no discernable impact on model predictions. The higher concentrations of aromatic hydrocarbons in the wholly evaporated experiments, as well as more constant initial CO concentrations, may explain why no relationship between model error and CO was observed. The reaction of aromatics will form large concentrations of HO_2 through the photolysis of secondary products such as aldehydes (Yu et al. 1997; Calvert et al., 2002),

and thus the proportional impact of the reaction of the hydroxyl radical and carbon monoxide on HO_2 formation, and therefore total experimental reactivity, will be lower in experiments with high aromatic concentration.

CB05 reproduces $\Delta(O_3\text{-NO})$ less accurately for wholly evaporated experiments than for headspace evaporated experiments, whereas SAPRC and the MCM show little variability in model error between injection mode with the exception of headspace experiments with high initial carbon monoxide. In previous appraisals CB05 has under-predicted ozone concentrations for chamber experiments containing aromatic hydrocarbons (Yarwood et al., 2005), and the poor performance of CB05 in wholly evaporated experiments compared to headspace experiments is therefore most likely due to the higher aromatic concentration.

Formaldehyde

One advantage of using detailed chemical mechanisms is that the formation of secondary products can be modelled and validated against experimental data. This is important for simulations of photochemical smog events where the concentration of organic species such as formaldehyde, acetaldehyde and peroxy acetyl nitrate (PAN) can reach levels harmful to human health (Dodge, 2000).

In these experiments formaldehyde was measured independently using both FTIR and DNPH-cartridge analysis and the average results at 6 hours for each method were within 20%, with the DNPH measurement used for comparison to model results. Formaldehyde was explicitly modelled in the MCM and SAPRC, however in CB05 some terminal alkenes were lumped into the FORM (formaldehyde) species initially.

Comparison of the model error for formaldehyde using SAPRC and the MCM is shown for headspace experiments and wholly evaporated experiments (Fig. 6). For both subsets of experiments the final formaldehyde concentration observed experimentally was similar, with averages of 39.1 ± 7.2 ppbv for headspace fuel experiments and 38.5 ± 3.2 ppbv for the wholly evaporated fuel experiments. The predictions of headspace vapours using SAPRC was slightly higher than observed, whereas it was 10% less for wholly evaporated experiments and all MCM predictions. Both mechanisms predict formaldehyde formation to within 15% of experimental values for the majority of experiments. Although predictions of secondary formaldehyde formation could not be obtained for CB05, the results indicate that the model error for formaldehyde is between -40 and -60%.

Ethanol

Comparison of predicted ethanol reaction between the MCM and CB05 mechanisms are shown in Fig. 7. For all experiments more ethanol had reacted in the MCM than in CB05 due to the higher total OH radical predictions. To evaluate the impact of ethanol oxidation in the SAPRC mechanism, the reaction of ethanol with OH was added as an explicit reaction to the base mechanism. The product yields were that used in the extended SAPRC-99 mechanism, with a corrected reaction rate of ethanol with OH used.

The addition of this reaction to the SAPRC mechanism (called SAPRC+ETOH mechanism) did not alter $\Delta(O_3\text{-NO})$ predictions substantially, with the total change in final concentration less than 2% for all experiments. Some differences were observed in the predictions of formaldehyde and acetaldehyde (Fig. 8). In the SAPRC lumping module, ethanol is lumped to the ALK3 analogue. Consistent with the change from ALK3 mechanism to specific ethanol degradation, the concentration of formaldehyde has decreased with an increase observed in the concentration of acetaldehyde. Although the acetaldehyde species in the SAPRC mechanism also contains glycolaldehyde and similar species, acetaldehyde could be compared favourably as the concentration of glycolaldehyde was expected to be low for these experiments.

For the SAPRC mechanism containing the explicit ethanol oxidation approximately 10% of the ethanol reacts over 6 hours, consistent with SAPRC and CB05 (Fig. 7). For the wholly evaporated experiments, approximately 15% of the ethanol had reacted by the end of the simulations. The concentration of ethanol reacted was related to the predicted OH concentration, which is much higher in the SAPRC wholly evaporated simulations than in the equivalent headspace experiments, and also in the equivalent MCM and CB05 predictions.

The lack of difference in the prediction of $\Delta(O_3\text{-NO})$ between the SAPRC mechanisms once ethanol has been added to the mechanism may be due to a number of factors. (1) The low reactivity of ethanol/ALK3 relative to more reactive olefins and aromatics. (2) Ozone formation in these experiments is not sensitive to ethanol oxidation due to high concentrations of reactive hydrocarbons. (3) There is an external radical source (HONO flux) which dominates the radical source balance. In other experiment types, the photolysis of aldehydes yielding HO_2 could dominate OH formation in the chamber and therefore changes in the aldehyde concentration may have a larger effect in other

experiments. (4) The aldehyde products react and photolyse similarly under these experimental conditions, or are not significantly different enough to produce a noticeable effect in ozone formation.

For these chamber experiments, the inclusion of an explicit ethanol species was determined to have little impact on total reactivity in the system. Some changes were observed on the predictions of individual aldehydes, however the sum of the concentrations of aldehydes remained similar.

Conclusion

The photooxidation of fuel vapours in a smog chamber was performed and simulated using three chemical mechanisms. Two different injection modes were used; headspace equilibrated evaporated fuel and wholly evaporated fuel. For each mode three fuel types were tested: unleaded petrol (ULP) and two ethanol blends (E5, E10).

The predictions of $\Delta(O_3\text{-NO})$ by the SAPRC mechanism were comparable to within 10% of the experimental data for both headspace and wholly evaporated experiments, with the exception of E5 headspace experiments with high initial CO. The predictions of $\Delta(O_3\text{-NO})$ by the MCM were an average of 16% lower than experimental values. For headspace experiments model error for all three mechanisms was relative to initial carbon monoxide, indicating a possible problem with mechanism predictions under similar conditions where high CO concentrations are present. Predictions of $\Delta(O_3\text{-NO})$ by CB05 were on average 34% lower than experimental values, and varied between injection modes with wholly evaporated experiments not as well predicted as headspace experiments. This difference is postulated to be due to higher aromatic content in the wholly evaporated experiments.

The ability of the mechanisms to predict other major products was also investigated. The formation of formaldehyde was well predicted by both SAPRC and the MCM, but indicative evidence indicates a large under-prediction using CB05. Ethanol was a major component of vapour from ethanol-blended experiments. Only small quantities of ethanol reacted, with only 10% predicted to have reacted by the MCM and the CB05 mechanism after 6 hours. The inclusion of ethanol as an explicitly represented species in the SAPRC mechanism altered the predictions of $\Delta(O_3\text{-NO})$ by less than 2%, however some differences were observed in the formaldehyde and acetaldehyde predictions.

In summary, the formation of ozone and other key products in smog chamber experiments of evaporated fuel was modelled using the Master Chemical Mechanism, the

SAPRC mechanism and the Carbon Bond mechanism. The ability of the SAPRC mechanism was adequate in predicting oxidant formation, although the radical balance in CB05 simulations was deemed too low to accurately replicate ozone formation.

Acknowledgements

The authors would like to thank the Department of the Environment, Water, Heritage and the Arts for funding for this project. The authors also acknowledge Anne Tibbett, Rosemary Wood and Michael Patterson for performing the aldehyde and hydrocarbon analyses. Peter Nancarrow provided assistance with the chamber experiments and Martin Cope and Robert Hynes helped with mechanism programming and construction, as well as valuable advice.

References

Angove, D.E., Fookes, C.J.R., Hynes, R.G., Walters, C.K., Azzi, M., 2006. The characterisation of secondary organic aerosol formed during the photodecomposition of 1,3-butadiene in air containing nitric oxide. Atmospheric Environment 40, 4597-4607.

Atkinson, R., 2000. Atmospheric Chemistry of VOCs and NO_x. Atmospheric Environment 34, 2063-2101.

Atkinson, R., Baulch, D.L., Cox, R.A., Crowley, J.N., Hampson, R.F., Hynes, R.G., Jenkin, M.E., Rossi, M.J., Troe, J., 2006. Evaluated kinetic and photochemical data for atmospheric chemistry: Volume II - gas phase reactions of organic species. Atmospheric Chemistry and Physics 6, 3625-4055.

Beer, T., 2001. Air Quality as a Meteorological Hazard. Natural Hazards 23, 157-169.

Bloss, C., Wagner, V., Jenkin, M.E., Volkamer, R., Bloss, W.J., Lee, J.D., Heard, D.E., Wirtz, K., Martin-Reviejo, M., Rea, G., Wenger, J.C., Pilling, M.J., 2005. Development of a detailed chemical mechanism (MCMv3.1) for the atmospheric oxidation of aromatic hydrocarbons. Atmospheric Chemistry and Physics 5, 641-664.

Calvert, J.G., Atkinson, R., Becker, K.H., Kamens, R.M., Seinfeld, J.H., Wallington, T.J., Yarwood, G., 2002. The Mechanisms of Atmospheric Oxidation of Aromatic Hydrocarbons. Oxford University Press, Oxford.

Carter, W.P.L., 2000. Documentation of the SAPRC-99 chemical mechanism for VOC reactivity assessment. Report to the California Air Resources Board, Contracts 92-329 and 95-308, May 8.

Carter, W.P.L., Atkinson, R., 1987. An Experimental Study of Incremental Hydrocarbon Reactivity. Environmental Science and Technology 21, 670-679.

Carter, W.P.L., Lurmann, F.W., 1991. Evaluation of a detailed gas-phase atmospheric reaction mechanism using environmental chamber data. Atmospheric Environment 25A, 2271-2806.

Carter, W.P.L., Malkina, I.L., 2002. Development and application of improved methods for measurement of ozone formation potentials of volatile organic compounds. Final report to the California Air Resources Board. Contract No. 97-314.

Carter, W.P.L., Smith, M., Duo, L., Malkina, I.L., Truex, T.J., Norbeck, J.M., 1999. Experimental Evaluation of Ozone Forming Potentials of Motor Vehicle Emissions. Final Report to California Air Resources Board Contract No. 95-903.

Carter, W.P.L., Cocker III, D.R., Fitz, D.R., Malkina, I.L., Bumiller, K., Sauer, C.G., Pisano, J.T., Bufalino, C., Song, C., 2005. A new environmental chamber for evaluation of gas-phase chemical mechanisms and secondary aerosol formation. Atmospheric Environment 39, 7768-7788.

Chu, P.M., Guenther, F.R., Rhoderick, G.C., Lafferty, W.J., 1999. The NIST Quantitative Infrared Database. Journal of Research of the National Institute of Standards and Technology 104, 59-81.

Cope, M.E., Hess, G.D., Lee, S., Tory, K., Azzi, M., Carras, J., Lilley, W., Manins, P.C., Nelson, P., Ng, L., Puri, K., Wong, N., Walsh, S., Young, M., 2004. The Australian Air Quality Forecasting System. Part I: Project Description and Early Outcomes. Journal of Applied Meteorology 43, 649-662.

CSIRO, Orbital Engine Corporation Australia, 2008. Evaluating the Health Impacts of Ethanol Blend Petrol. Final Report to Department of the Environment, Water, Heritage and the Arts. Report No. KW48/17/F3.3F. Available at: http://www.environment.gov.au/atmosphere/fuelquality/publications/ethanol-health-impacts.html

Dodge, M.C., 2000. Chemical oxidant mechanisms for air quality modeling: critical review. Atmospheric Environment 34, 2103-2130.

Finlayson-Pitts, B.J., Pitts, J., J.N., 1997. Tropospheric Air Pollution: Ozone, Airborne Toxics, Polycyclic Aromatic Hydrocarbons, and Particles. Science 276, 1045-1052.

Gasca, J., Ortiz, E., Castillo, H., Jaimes, J.L., González, U., 2004. The impact of liquefied petroleum gas usage on air quality in Mexico City. Atmospheric Environment 38, 3517-3527.

Geiger, H., Kleffmann, J., Wiesen, P., 2002. Smog chamber studies on the influence of diesel exhaust on photosmog formation. Atmospheric Environment 36, 1737-1747.

Griffith, D.W.T., 1996. Synthetic Calibration and Quantitative Analysis of Gas-Phase FT-IR Spectra. Applied Spectroscopy 50, 59-70.

Grosjean, E., Grosjean, D., 1998. Formation of Ozone in Urban Air by Photochemical Oxidation of Hydrocarbons: Captive Air Experiments in Porto Alegre, RS. Journal of the Brazilian Chemical Society 9, 131-143.

Hanst P.L., Hanst, S.T., 1993. Infrared Spectra for Quantitative Analysis of Gases. Infrared Analysis Inc., Anaheim, CA. Available at: http://www.infraredanalysisinc.com/

Hynes, R.G., Angove, D.E., Saunders, S.M., Haverd, V., Azzi, M., 2005. Evaluation of two MCM v3.1 alkene mechanisms using indoor environmental chamber data. Atmospheric Environment 39, 7251-7262.

Jenkin, M.E., Saunders, S.M., Pilling, M.J., 1997. The tropospheric degradation of volatile organic compounds: A protocol for mechanism development. Atmospheric Environment 31, 81-104.

Johnson, G.M., 1983. Factors Affecting Oxidant Formation in Sydney Air, In: Carras, J.N., Johnson, G.M. (Eds.), The Urban Atmosphere – Sydney, a Case Study, CSIRO, Melbourne, pp. 393-408.

Luecken, D.J., Phillips, S., Sarwar, G., Jang, C., 2008. Effects of using the CB05 vs. SAPRC99 vs. CB4 chemical mechanism on model predictions: Ozone and gas-phase photochemical precursor concentrations. Atmospheric Environment 42, 5805-5820.

Nguyen, H.T.-H., Takenaka, N., Bandow, H., Maeda, Y., de Oliva, S.T., Botelho, M.M.f., Tavares, T.M., 2001. Atmospheric alcohols and aldehyde concentrations measured in Osaka, Japan and in Sao Paulo, Brazil. Atmospheric Environment 35, 3075-3083.

Pereira, P.A.P., Santos, L.M.B., Sousa, E.T., Andrade, J.B., 2004. Alcohol- and Gasohol-Fuels: A Comparative Chamber Study of Photochemical Ozone Formation. Journal of the Brazilian Chemical Society 15, 646-651.

Rohrer, F., Bohn, B., Brauers, T., Brüning, D., Johnen, F.-J., Wahner, A., Kleffmann, J., 2005. Characterisation of the photolytic HONO-source in the atmosphere simulation chamber SAPHIR. Atmospheric Chemistry and Physics 5, 2189-2201.

Rothman, L.S., Jacquemart, D., Barbe, A., Chris Benner, D., Birk, M., Brown, L.R., Carleer, M.R., Chackerian Jr, C., Chance, K., Coudert, L.H., Dana, V., Devi, V.M., Flaud, J.-M., Gamache, R.R., Goldman, A., Hartmann, J.-M., Jucks, K.W., Maki, A.G., Mandin, J.-Y., Massie, S.T., Orphal, J., Perrin, A., Rinsland, C.P., Smith, M.A.H., Tennyson, J., Tolchenov, R.N., Toth, R.A., Vander Auwera, J., Varanasi, P., Wagner, G., 2005. The HITRAN 2004 molecular spectroscopic database. Journal of Quantitative Spectroscopy & Radiative Transfer 96, 139-204.

Schifter, I., Vera, M., Díaz, L., Guzmán, E., Ramos, F., López-Salinas, E., 2001. Environmental Implications on the Oxygenation of Gasoline with Ethanol in the Metropolitan Area of Mexico City. Environmental Science and Technology 35, 1893-1901.

Syomin, D.A., Finlayson-Pitts, B.J., 2003. HONO decomposition on borosilicate glass surfaces: implications for environmental chamber studies and field experiments. Physical Chemistry Chemical Physics 5, 5236-5242.

Utembe, S.R., Jenkin, M.E., Derwent, R.G., Lewis, A.C., Hopkins, J.R., Hamilton, J.F., 2005. Modelling the ambient distribution of organic compounds during the August 2003 ozone episode in the southern UK. Faraday Discussions 130, 311-326.

Watson, J.G., Chow, J.C., Fujita, E.M., 2001. Review of volatile organic compound source appointment by chemical mass balance. Atmospheric Environment 35, 1567-1584.

Yarwood, G., Rao, S., Yocke, M., Whitten, G.Z., 2005. Updates to the Carbon Bond Chemical Mechanism: CB05. Final Report to the US EPA, RT-0400675, December 8.

Yu, J., Jeffries, H.E., Sexton, K.G., 1997. Atmospheric Photooxidation of Alkylbenzenes - I. Carbonyl Product Analyses. Atmospheric Environment 31, 2261-2280.

List of Tables

Table 1. Comparison of ethanol reactivity and product yield between the three chemical mechanisms. Rates are calculated in 10^{-12} cm^3 $molecule^{-1}$ s^{-1}

Mechanism	Rate at 298 °K	Rate at 303 °K	CH_3CHO	HO_2	RO_2a	HCHO	RCHO
MCM	3.27	3.28	88.7%	88.7%	11.3%	-	-
SAPRC	3.31[b]	3.22[b]	96.0%	95.0%	5.0%	8.1%	-
CB05	3.19	3.23	90.0%	100.0%	10.0%	10.0%	5.0%

[a] RO_2: HOCH2CH2O2 in MCM, RO2-R in SAPRC and XO2 in CB05.

[b] This is the incorrect rate for SAPRC. For the temperature corrected rate the reaction rate of ethanol with OH is identical to that used in the MCM to 3 significant figures.

Table 2. Auxiliary mechanism for CSIRO smog chamber

Reaction	Rate
hv + wall → HONO	$J_{NO2} \times (4 \times 10^{-3})$ ppbv
NO_2 → α × HONO + (1 – α) × $wHNO_3$	1.2×10^{-6} s^{-1}
α	0.42
N_2O_5 → 2 × $wHNO_3$	1.0×10^{-5} s^{-1}
$N_2O_5 + H_2O$ → 2 × $wHNO_3$	$[H_2O] \times 10^{-20}$ cm^3 $molec^{-1}$ s^{-1}
O_3 → wall	2.0×10^{-7} s^{-1}
OH → HO_2	4.17 s^{-1}
HNO_3 → $wHNO_3$	3.3×10^{-6} s^{-1}
$wHNO_3$ → NO_2 + OH	-[a]
Injector → HONO	1.5 ppbv $hour^{-1}$

[a] Rate previously included but was removed for this work.

Table 3. Δ(O_3-NO) model error (%) for headspace (HS) and wholly evaporated (WE) experiments. The model error represents the difference between replicate experiments.

Mechanism	HS ULP	HS E5	HS E10	WE ULP	WE E5	WE E10
SAPRC	-1.5 ± 5.7	15.7 ± 2.6	-2.3 ± 5.9	-4.1 ± 0.9	-2.5 ± 0.3	0.4 ± 3.1
MCM	-17.0 ± 4.7	-4.8 ± 2.1	-19.9 ± 4.9	-16.0 ± 0.6	-20.6 ± 0.2	-19.0 ± 2.5
CB05	-27.1 ± 3.8	-17.2 ± 1.7	-28.8 ± 4.0	-44.1 ± 0.6	-44.8 ± 0.2	-43.7 ± 1.4

Figures

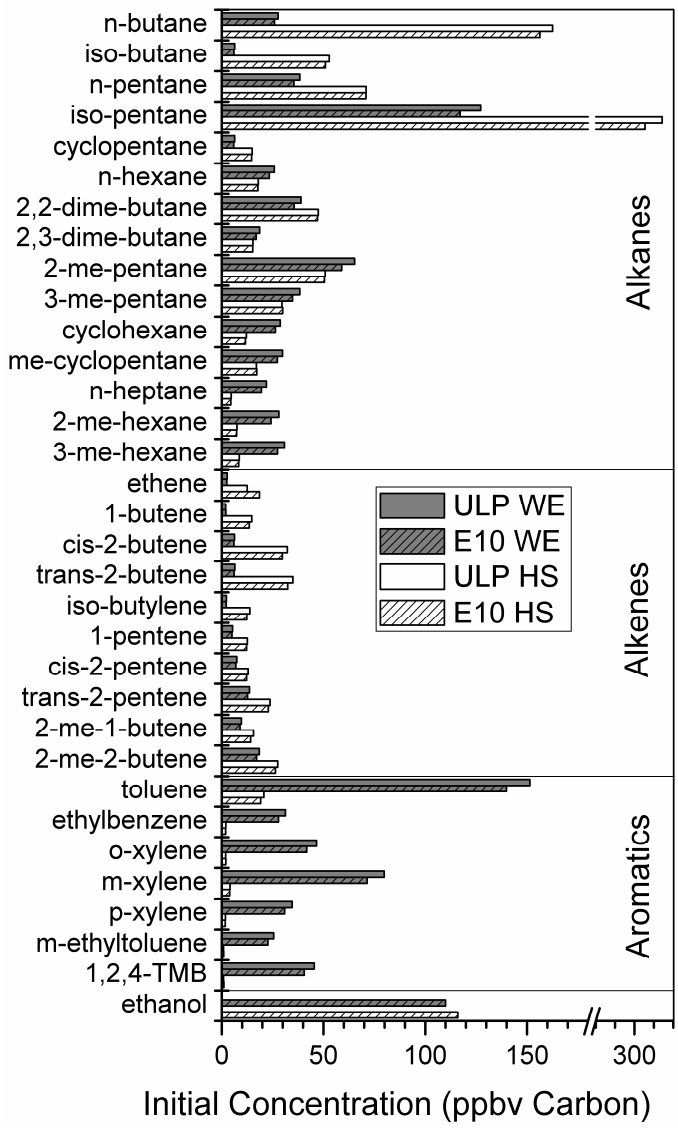

Fig. 1. Average initial concentration of important VOCs for wholly evaporated (WE) and headspace evaporated (HS) experiments. Comparison has been shown for ULP and E10 experiments.

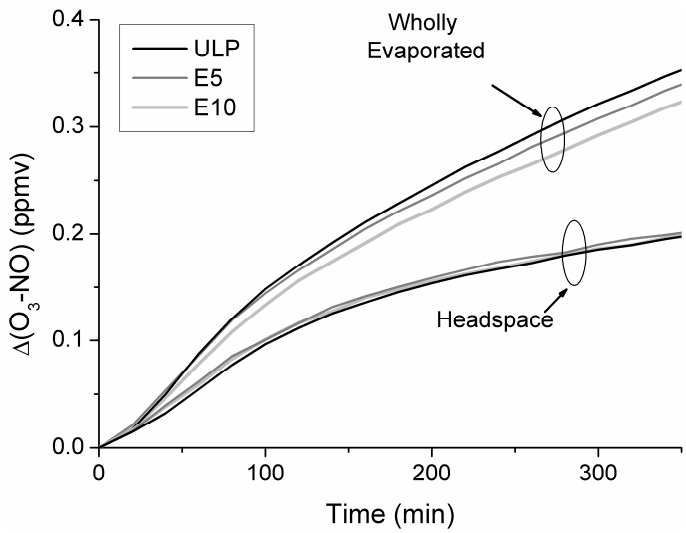

Fig. 2. Comparison of average experimental $\Delta(O_3\text{-NO})$ for wholly evaporated and headspace vapour experiments.

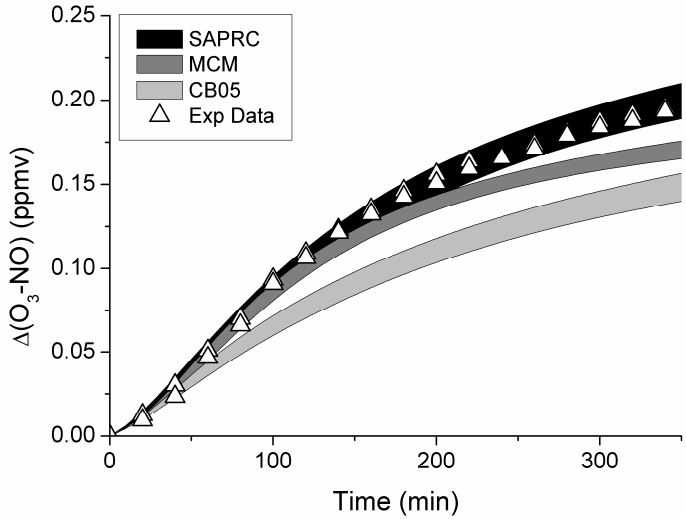

Fig. 3. Effect of HONO flux rate on mechanism predictions for a ULP headspace evaporated experiment.

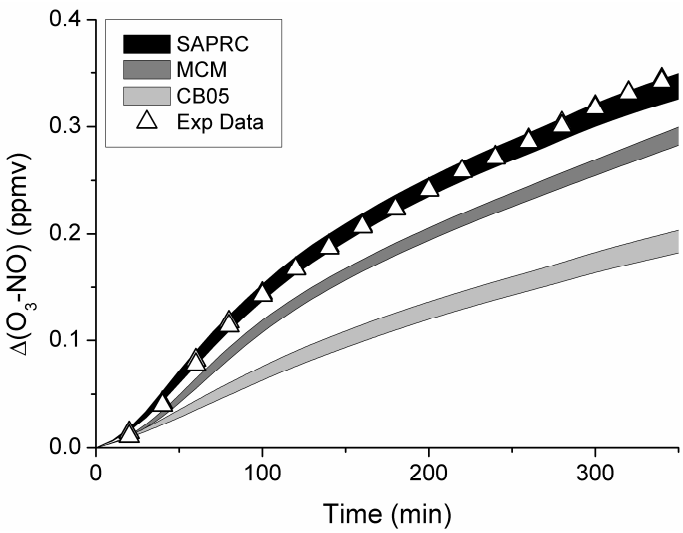

Fig. 4. Effect of HONO flux rate on mechanism predictions for a ULP wholly evaporated experiment

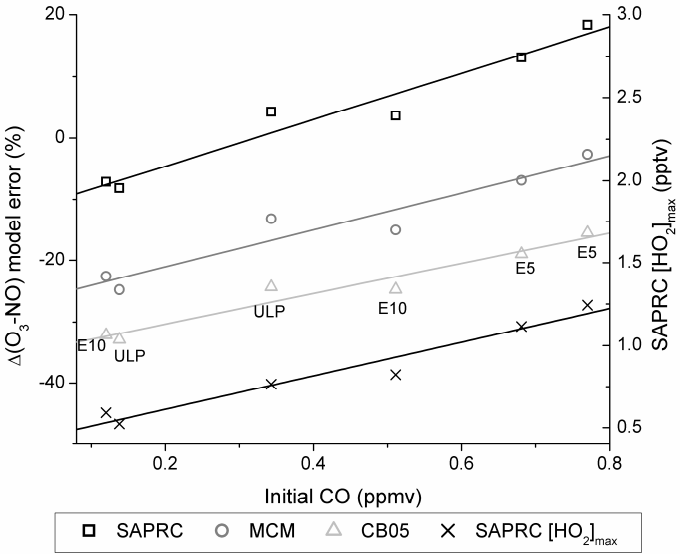

Fig. 5. $\Delta(O_3\text{-NO})$ model error for headspace vapour experiments relative to initial carbon monoxide concentration. The maximum HO_2 concentration as predicted by the SAPRC mechanism is also shown in parts per trillion.

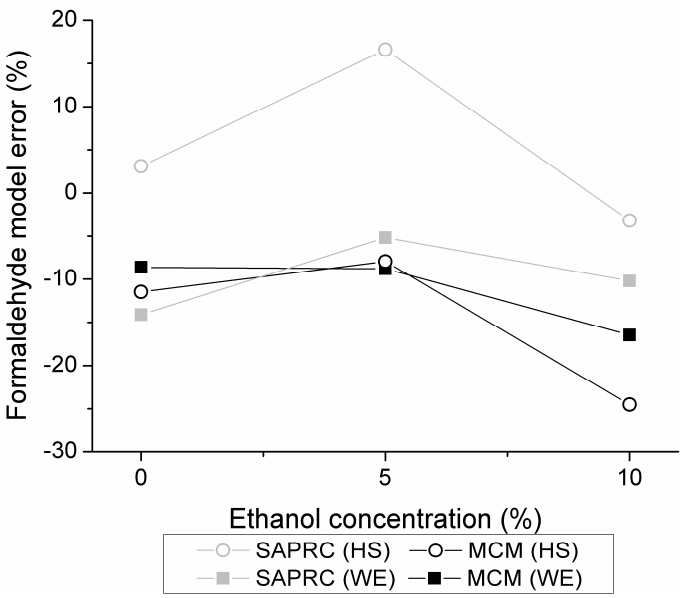

Fig. 6. Formaldehyde model error for headspace (HS) and wholly evaporated (WE) experiments

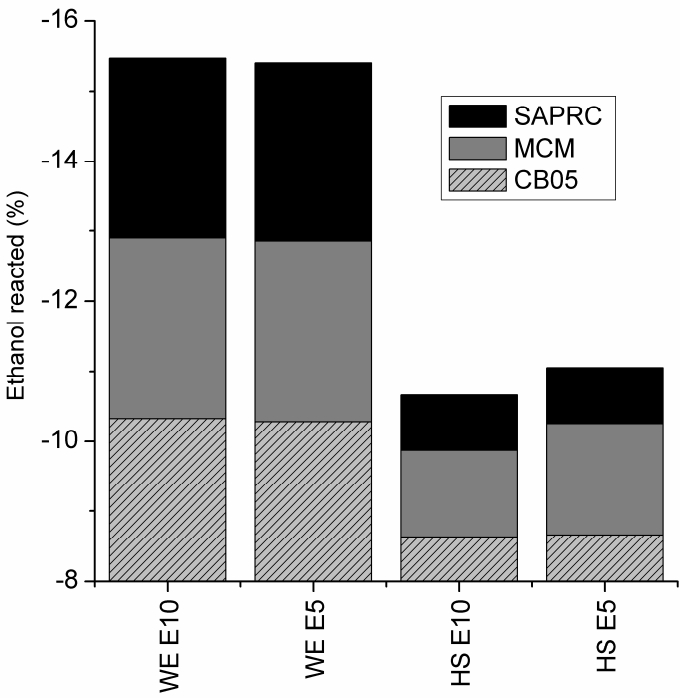

Fig. 7. Concentration of ethanol reacted in the MCM, CB05 and SAPRC+ETOH mechanisms.

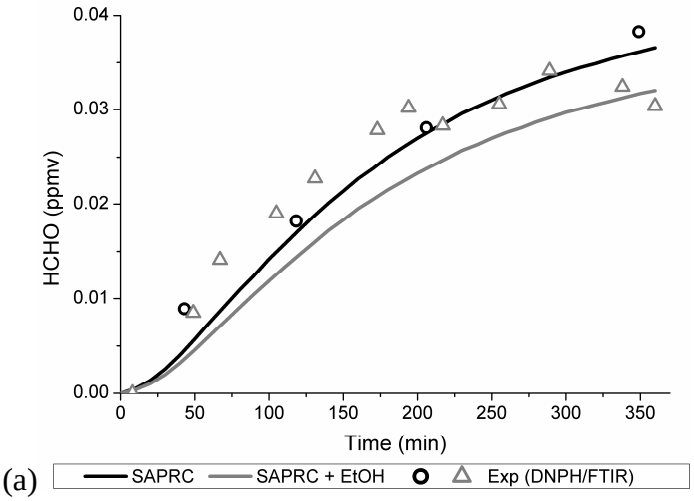
HCHO (ppmv)
0.04
0.03
0.02
0.01
0.00
0
50
100
150
200
250
300
350
Time (min)
SAPRC
SAPRC + EtOH
Exp (DNPH/FTIR)

(a)

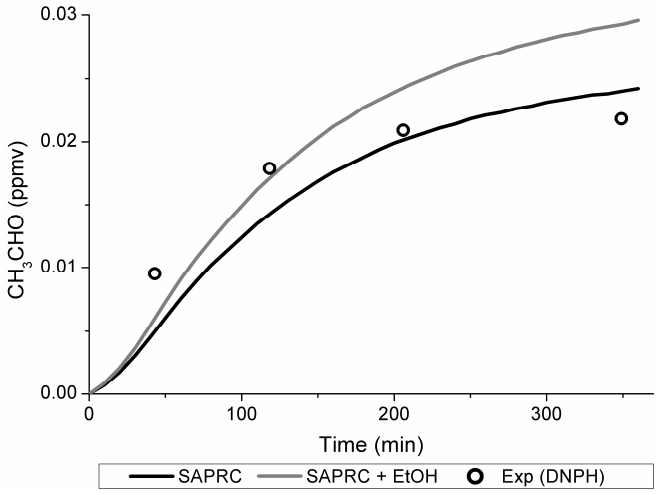
CH3CHO (ppmv)
0.03
0.02
0.01
0.00
0
100
200
300
Time (min)
SAPRC
SAPRC + EtOH
Exp (DNPH)

(b)

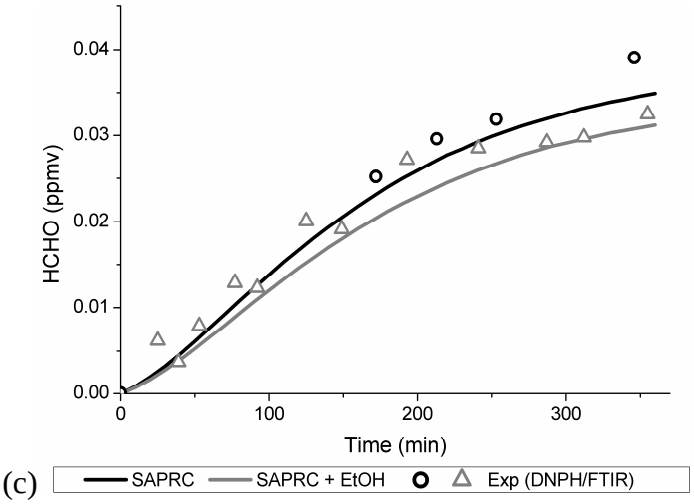
HCHO (ppmv)
0.04
0.03
0.02
0.01
0.00
0
100
200
300
Time (min)
SAPRC
SAPRC + EtOH
Exp (DNPH/FTIR)

(c)

(d)

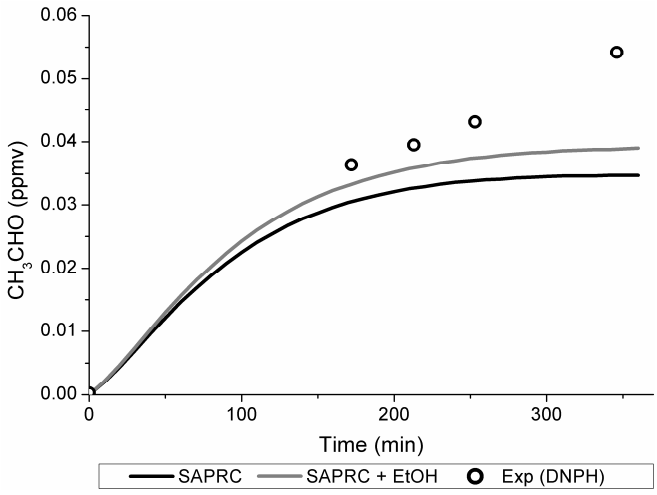

Fig. 8. Formaldehyde and acetaldehyde predictions for SAPRC and SAPRC+ETOH mechanism for (a,b) E10 wholly evaporated experiment and (c,d) E10 headspace evaporated experiment